THE JOURNAL OF PHYSICAL CHEMISTRY B

ARTICLE

pubs.acs.org/JPCB

Effective Improvement of Water-Retention in Nanocomposite Membranes Using Novel Organo-Modified Clays as Fillers for High Temperature PEMFCs

Isabella Nicotera,*[,†] Apostolos Enotiadis,[‡] Kristina Angjeli,[†] Luigi Coppola,[†] Giuseppe A. Ranieri,[†] and Dimitrios Gournis[‡]

[†]Department of Chemistry, University of Calabria, 87036 Rende, Cosenza, Italy

[‡]Department of Material Science and Engineering, University of Ioannina, 45110 Ioannina, Greece

Supporting Information

ABSTRACT: Toward an enhanced water-retention of polymer electrolyte membranes at high temperatures, novel organo-modified clays were prepared and tested as fillers for the creation of hybrid Nafion nanocomposites. Two smectite clays (Laponite and montmorillonite), with different structural and physical parameters, were loaded with various cationic organic molecules bearing several hydrophilic functional groups ($-NH_2$, $-OH$, $-SO_3H$) and incorporated in Nafion by solution intercalation. The resulted hybrid membranes were characterized by a combination of powder X-ray diffraction, FTIR spectroscopy, and thermal analysis (DTA/TGA) showing that highly homogeneous exfoliated nanocomposites were created where the individual organoclay layers are uniformly dispersed in the continuous polymeric matrix. In this paper, water-transport properties were investigated by NMR spectroscopy, including pulsed-field-gradient spin−echo diffusion and spectral measurements conducted under variable temperature. Organo-montmorillonite nanofillers demonstrate a considerable effect on the Nafion polymer in terms both of water absorption/retention and water mobility with a remarkable behavior in the region of high temperatures (100−130 °C), denoting that the surface modifications of this clay with acid organic molecules significantly improve the performance of the final composite membrane. ^{1}H NMR spectral analysis allowed a general description of the water distribution in the system and an estimation of the number of water molecules involved in the hydration shell of the sulfonic groups as well as that absorbed on the organoclay particles.

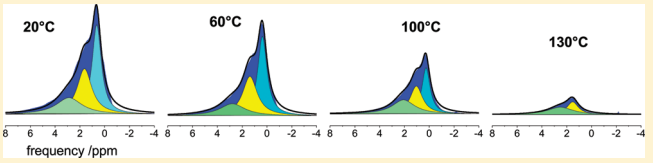

1. INTRODUCTION

Proton exchange membrane fuel cells (PEMFCs) are promising candidates for both vehicle applications and local on-site power generation system in the future, due to their high energy efficiency as well as high power density, even at relatively low operation temperatures. The electrolyte in these systems is a proton conducting polymer membrane. The development of high-performance electrolyte membrane is critical to achieve the optimal power density and efficiency of a PEMFC. In fact, the ohmic loss of the membrane is one of the most significant cause of overpotential in the fuel cell operational current range. PEMFCs operating in the typical 60−80 °C temperature range face problems including poor carbon monoxide (from reformed hydrogen or methanol as fuels) tolerance and heat rejection. These drawbacks can be overcome by increasing the operation temperature range up to 110−130 °C,[1,2] but this leads to an unacceptable decrease in the proton conductivity of the electrolyte due to water loss.[3] As a rule, the following properties of polymeric membranes need to be optimized for use in fuel cells: (1) high proton conduction; (2) good mechanical, chemical and thermal strength requiring the selection of suitable polymer backbone; (3) low gas permeability, which is dependent on material and thickness of the membrane.

Nafion (a registered trademark of E. I. du Pont de Nemours and Co.) is the electrolyte that has been most extensively studied in PEMFC applications. However, the most significant barrier to run such polymer electrolyte fuel cell at elevated temperatures is maintaining the proton conductivity of the membrane, which depends critically on the presence of water: the conductivity of a dry membrane is several orders of magnitude lower than that of a fully saturated membrane. According to the literature several membrane properties may benefit from the presence of homogeneously dispersed organic/inorganic fillers such as hygroscopic inorganic oxide (SiO_2, TiO_2, ZrO_2), zeolite, heteropoly acids, and zirconium hydrogen phosphate to enhance the water retention property.[3−13]

Recent studies have shown that polymer nanocomposites based on layered clay nanoparticles exhibit reduced gas permeability due to the presence of impermeable clay platelets as well as

Received: March 30, 2011
Revised: June 8, 2011
Published: June 14, 2011

Table 1. Organic Molecules Used for the Chemical Modification of SWy and Lap Clays

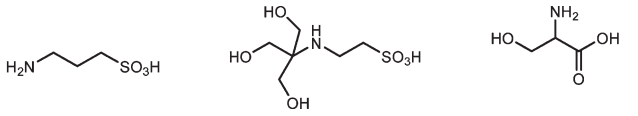

SULF	TES	SER
3-amino-1 propanesulfonic acid	2-{[2-hydroxy-1,1 bis(hydroxymethyl) ethyl]aminoethanesulfonic acid	2-Amino-3-hydroxypropionic acid (or Serine)

structural changes in the polymer induced by the clay nanofillers.[14−16] Among layered silicates, smectite clays are attractive candidates as Nafion additives because of their nanometer size, proton conductivity, good thermal stability and potential to reduce fuel (e.g., methanol) permeability.[17,18] Smectite clays are a class of layered aluminosilicate minerals with a unique combination of swelling, intercalation, and ion exchange properties. They consist of an octahedral alumina layer fused between two tetrahedral silica layers (about 1 nm).[19,20] The monovalent ions located between the clay layers allow the absorption of polar solvent, like water, with good retention capacity so, when incorporated into a polymer membrane, they help to prevent the loss of the hydration water not only at high temperatures but also under low relative humidity environment. The charge on the layers affects many fundamental properties of the clays, including water holding (an important property for the creation of Nafion nanocomposite membrane), cation fixation, swelling ability, cation exchange capacity, and high surface area. Moreover, the properties of the smectite nanoclays can be tailored using simple chemical methods such as intercalation with organic or inorganic guest molecules. Their surface properties, for example, can be easily modified through treatment with an organic surfactant. As a result the presence of the surfactant expands the interlayer gallery rendering the nanoclay compatible with hydrophobic media and polymer matrices. Because of their distinctive structure and properties, these organic−inorganic hybrid materials (so-called "organo-clays") can be utilized in a wide variety of applications including, construction of modified electrodes, biosensors or biocatalysts,[21−23] adsorbents for environmental remediation (e.g., removal of heavy metal ions for water[24]) but also as nanofillers for polymer reinforcement.[25−27] Thus, a strategy toward the improvement of the water retention of the Nafion membrane is the incorporation in the polymer matrix hybrid nanofillers of modified clays bearing organic functionalities with high affinity for Nafion and increased sites for water trapping.

In the present work, various organo-modified clays were prepared and tested as nanofillers for the creation of novel hybrid Nafion composites. The clays used were a synthetic clay (Laponite) with low layer charge density and small particle size (20 nm), and a natural montmorillonite (SWy-2) with medium layer charge density and high particle size (200 nm). Three cationic organic molecules, 3-amino-1-propanesulfonic acid, 2-{[2-hydroxy-1,1-bis(hydroxymethyl) ethyl]amino}ethanesulfonic acid and serine, were used for the clay modification and the resulting organo-modified derivatives were incorporated in Nafion by solution intercalation (membranes with pristine clays were also synthesized for comparison). The modification is based on the functionalization of the clay surfaces by various functional groups ($-NH_2$, $-OH$, $-SO_3H$) that can effectively (1) increase the concentration of acidic (hydrophilic) functional groups (sulfonic, hydroxyl, etc.) on the surfaces of the clay minerals and thus improve the proton conductivity through the membrane and, (2) enhance their compatibility with polymeric materials, since silicate clays are hydrophilic and have little affinity for hydrophobic polymers like the hydrophobic phase of Nafion.

The organofillers and the nanocomposite membranes were investigated by a combination of powder X-ray diffraction, FTIR spectroscopy and thermal analysis (DTA/TGA) while the characteristics of the membranes were studied in terms of morphological analysis by scanning electronic microscopy (SEM), and, mainly, in terms of transport properties by NMR spectroscopy, in order to study of the water dynamics inside the electrolyte membranes, which is one of the key aspects in the evaluation of these materials.[10,28−31] For this purpose the pulse-field-gradient spin−echo NMR (PFGSE-NMR) method[32] was employed in this work to obtain a direct measurement of water self-diffusion coefficients on the water-swelled membranes in a wide temperature range (25−130 °C). This technique together with the ^{1}H NMR spectra have provided a general description of the water behavior: how it is shared in the polymer structure, effects of the nanofillers and their surface modifications, interactions between water molecules and hydrophilic groups present and, finally, a quantitative estimate of the hydration number, i.e., number of water molecules solvating the hydrophilic sites both in the maximum hydration regime and in quasi-dehydration conditions.

2. EXPERIMENTAL SECTION

2.1. Materials. Two smectite clays with different structural and physical parameters (structural formula, particle size and cation exchange capacity) were used.[33,34] The first was a natural Wyoming montmorillonite (SW_y-2) obtained from the Source Clay Minerals Repository, University of Missouri (Columbia), with a cation exchange capacity (CEC) measured by the Co(II) procedure equal to 80 mequiv per 100 g of clay and particle size around 200 nm. The second clay was a synthetic trioctahedral hectorite, Laponite (Lap), produced by Laporte Industries Ltd. with a CEC of 48 mequiv per 100 g clay and a particle size of 20 nm. SWy-2 montmorillonite was fractioned to <2 μm by gravity sedimentation and purified by well-established procedures in clay science.[35] Sodium-exchanged samples (Na^+-SW_y-2) were prepared by immersing the clay into 1 N solution of sodium chloride. Cation exchange was complete by washing and centrifuging four times with dilute aqueous NaCl. The samples were finally washed with distilled deionized water and transferred into dialysis tubes in order to obtain chloride-free clays and then dried at room temperature.

For the chemical modification of the pristine clays three organic molecules were used: 3-amino-1-propanesulfonic acid (SULF), 2-{[2-hydroxy-1,1-bis(hydroxymethyl) ethyl]amino}ethanesulfonic acid (TES) and serine (SER). Their structural formulas are shown in Table 1.

dx.doi.org/10.1021/jp202954g |J. Phys. Chem. B 2011, 115, 9087–9097

Finally, Nafion solution (20 wt % in mixture of lower aliphatic alcohols and water) and *N*,*N*-dimethylformamide (DMF)) were purchased from Aldrich and used as received.

2.2. Preparation of Organo-Modified Clay Nanofillers. For the preparation of the organoclays, aqueous 1 wt % clay suspensions were reacted under vigorous stirring with aliquots of the above organic molecules solutions in water such that the amount of the cationic molecule added to corresponds three times the CEC of the clay. The mixtures were stirred for 24 h, centrifuged, washed with water, and air-dried by spreading on glass-plates. The products are designated as follows: SWy/TES, SWy/SER, and SWy/SULF and Lap/TES, Lap/SER, and Lap/SULF.

2.3. Composites Membranes Preparation. The composite membranes were prepared from 20 wt % Nafion solution according to the following processes: (i) 1 g of Nafion solution was heated at about 60 °C to remove all the solvents (water, 2-propanol, etc.); (ii) Nafion resin was redissolved with 10 mL of DMF until become a clear solution; (iii) the filler was dispersed in the same solvent under stirring for 1 day and then added slowly to the solution of Nafion; (iv) the final solution was ultrasonicated for 1 h and then stirred at 60 °C to ensure complete mixing; finally (v) casting on a Petri dish at 80 °C overnight was performed in order to obtain a homogeneous membrane. The hybrid membrane is removed from the petri dish by immersing the glass plate in deionized water for several minutes. In order to reinforce the membrane, this was sandwiched and pressed between two Teflon plates and put in oven at 150 °C for about 15 min. All composite membranes produced by casting were subsequently treated by rinsing in: (i) boiling HNO_3 solution (1 M) for 1 h to oxidize the organic impurities, (ii) boiling H_2O_2 (3 vol %) for 1 h in order to remove all the organic impurities, (iii) boiling deionized H_2O for 40 min three times, (iv) boiling H_2SO_4 (0.5 M) for 1 h min to remove any metallic impurities, and again (v) boiling deionized H_2O for 40 min twice to remove excess acid. According to McMillan et al.[36] an ulterior purification procedure was performed in order to ensure the removal of paramagnetic contaminants which are particularly damaging to an NMR experiment, such as the presence of copper that we found by electron paramagnetic resonance analysis. By this procedure membranes were soaked in EDTA solution (0.001 M) for 1 day after followed by a thorough rinse. Then soaked in 2 M HCl at a temperature of 80 °C for 2 h followed by boiling in fresh distilled−deionized water to remove any residual acids and again repeated the treatment with EDTA. Finally, rinsing in boiled deionized water three times to remove residual EDTA and stored at room temperature at fully hydrated state.

2.4. Characterization Techniques. The X-ray powder diffraction data were collected on a D8 Advanced Bruker diffractometer by using Cu Ka (40 kV, 40 mA) radiation and a secondary beam graphite monochromator. The patterns were recorded in a 2θ range from 2° to 40°, in steps of 0.02° and counting time 2 s per step. Infrared spectra were measured with a FT-IR 8400 spectrometer, in the region of 400−4000 cm^{-1}, equipped with a DTGS detector. Each spectrum was the average of 32 scans collected at 2 cm^{-1} resolution. Samples were in the form of KBr pellets containing ca. 2 wt % samples while membranes measured as received. Thermogravimetric (TGA) and differential thermal (DTA) analysis were performed using a Perkin-Elmer Pyris Diamond TG/DTA. Samples of approximately 5 mg were heated under air from 25 to 850 °C, at a rate of 10 °C/min. The morphological studies were performed by using a QUANTA FEG 400 F7, FEI microscope operating in the e-SEM mode. The SEM images were acquired collecting the backscattered electrons induced by using 10 keV electron beam and 0.4 mbar of water humidity.

NMR measurements were performed on a Bruker NMR spectrometer AVANCE 300 Wide Bore working at 300 MHz on ^1H. The employed probe was a Diff30 Z-diffusion 30 G/cm/A multinuclear with substitutable RF inserts. The spectra were obtained by a single $\pi/2$ pulse sequence. The NMR pulsed field gradient spin−echo (PFG-SE) method[32] was used to measure self-diffusion coefficients. This technique consists of two rf pulses, Hahn-echo sequence $(\pi/2-\tau-\pi)$, with two identical pulsed-field gradients, the first applied between the 90° and 180° rf pulse (during the dephasing) and the second after the 180° rf pulse (during the rephasing) but before the echo. Following the usual notation, the pulsed-field gradients have magnitude g, duration δ, and time delay Δ (different from the degree of ionic association). The attenuation of the echo amplitude is represented by the Stejskal-Tanner equation:

$$A(g) = A(0)\, exp[-\gamma^2 g^2 D\delta^2(\Delta - (\delta/3)]$$

where D is the self-diffusion coefficient and γ is the nuclear gyromagnetic ratio and $A(0)$ is the amplitude of the echo at $g = 0$. Note that the exponent in the equation is proportional to the mean-squared displacement of the molecules over an effective time scale $(\Delta - (\delta/3))$. For the investigated samples, the experimental parameters, Δ and δ, are 10 and 1 ms, respectively. The gradient amplitude, g, varied from 10 to 600 G cm^{-1}. In this condition the uncertainty in the self-diffusion measurements is ∼3%. It is worth noting that a Gaussian self-diffusion of water (i.e., not restricted diffusion) has been observed also for a diffusion time (Δ) longer than 40 ms. (See the Supporting Information, Figure S1).

Both self-diffusion and spectra measurements were conducted by increasing temperature step by step from 20 to 130 °C, with steps of 20 K, and leaving the sample to equilibrate for about 20 min.

Prior to the NMR measurements, membranes were dried in oven, weighed and then immersed in distilled water at room temperature. Upon being removed from the water they were quickly blotted dry with a paper tissue (to eliminate most of the free surface liquid). The water content value was determined using a microbalance and recorded as:

$$\text{uptake } \% = [(m_{wet} - m_{dry})/m_{dry}] \times 100$$

At this point, the membranes were loaded into a 5 mm NMR Pyrex tube and hermetically sealed.

3. RESULTS AND DISCUSSION

3.1. Structural Investigation. For the surface modification of the parent smectite clays a simple procedure was followed. Positively charged molecules are introduced into interlayer space of layered clay minerals by ion exchange procedure where charge balancing cations (e.g., Na^+) are replaced by the organic cations. The introduced organic cations are held strongly by electrostatic forces with the negatively charged clay surfaces and the final conformation depends on the shape, size, and total charge of the organic cations and also on the charge density of the clay surface. In our case, the intercalation procedure involves

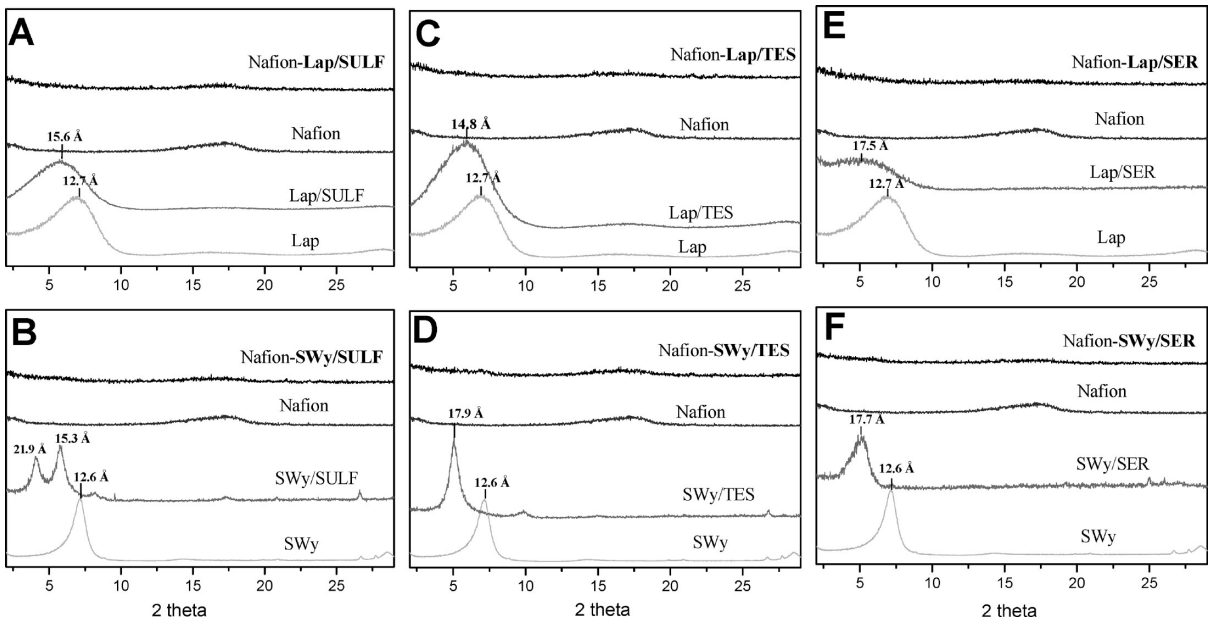

Figure 1. XRD patterns of pristine clays, organo-modified clays, filler-free Nafion and nanocomposite membranes with 3 wt % organoclay nanofillers.

an initial pre-equilibrium reaction in which the primary (SULF and SER) or secondary (TES) amino groups of the organic molecules are protonated:

where: (i) for SULF R_1: $-(CH_2)_3SO_3H$ and R_2: -H;
(ii) for TES R_1: $-(CH_2)_2SO_3H$ and R_2: $-C(CH_2OH)_3$
(iii) for SER R_1: $-C(CH_2OH)(COOH)$ and R_2: -H

The protonated organic molecules were readily adsorbed on the clay surfaces, by ion exchange. The monovalent Na^+ exchangeable cations are replaced easily by the protonated amino molecules according to the following reaction:

where the bold lines represent the clay platelets.

X-ray diffraction (XRD) measurements provide a powerful tool to understand not only the changes in the interior of the clay microenvironment, and thus reveal the successful modification of the parents nanoclays, but also to evaluate the type of composites created after the incorporation of the hybrid layered fillers in the Nafion matrix. Figure 1 shows in comparison the XRD patterns of pristine clays before and after the intercalation of the organic molecules as well as the filler-free Nafion and the nanocomposites prepared with the organoclays at 3 wt % filler to polymer loading. The XRD data show an increase of the basal spacing (d_{001}) of both clays after insertion of the three guest materials. More specifically, in the case of Laponite samples, the basal spacing d_{001}, which is 12.7 Å in the pristine clay, becomes 15.6, 14.8, and 17.5 Å in the modified clays with SULF, TES, and SER, respectively. If we consider that the thickness of a clay layer is 9.6 Å,[37] these values correspond to intersheet separations (L) of 6.0, 5.2, and 7.9 (where $L = d_{001} - 9.6$ Å) for Lap/SULF, Lap/TES, and Lap/SER, respectively. This increment in the interlayer space is indicative of the intercalation of the three cationic molecules into the Laponite interlayers where the guest molecules adopts an inclined orientation (at a certain angle) between the clay surfaces. The XRD results for the other organoclays with SWy-2 montmorillonite are analogous with the increment in the *d*-spacing to be more pronounced. XRD patterns of SWy/TES and SWy/SER show d_{001} spacings of 17.9 and 17.7 Å, which corresponds to intersheet separations of 8.3 and 8.1 Å, respectively. These higher *d*-spacings of the montmorillonite organoclays implying that the organic cations are lying in the interlayer space of the mineral in a more upward position (higher angle) compared with the corresponding organoclays with Laponite. This is probably due to the higher CEC of montmorillonite compared to Laponite which designates that the amount of intercalated molecules is much higher in the case of montmorillonite leading to higher *d*-spacings compared to Laponite samples. Finally, when the montmorillonite clay was treated with SULF solution (SWy/SULF), two d_{001} spacings are observed at 21.6 Å (Δ = 12.0 Å) and 15.5 Å (Δ= 5.9 Å) arising from two different conformations of the SULF cations within the clay layers. The intersheet separation of 12.0 Å is probably due to the formation of a double-layer arrangement of the SULF molecules in the interlayer space while the value of 5.9 Å—which is almost half of the previous one—arises from the formation of a single layer arrangement. Similar mixed phases have been observed during the intercalation of organic surfactants (alkylammonium derivatives)[38,39] or other polar molecules such as ethylene glycol.[40]

Moreover, the XRD patterns (Figure 1) of all nanocomposite membranes show clearly a broad band centered at 17° distinctive of the Nafion polymer arrangement.[41,42] The absence of the d_{001} diffraction peak, characteristic of the

dx.doi.org/10.1021/jp202954g |J. Phys. Chem. B 2011, 115, 9087–9097

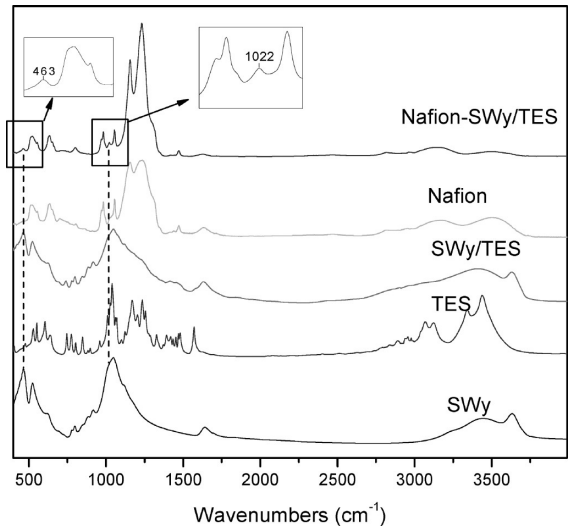

Figure 2. FT-IR spectra of pristine (SWy) clay, TES surfactant, SWy/TES organoclay, filler-free Nafion, and nanocomposite membrane with 3 wt % SWy/TES.

modified clays, in the patterns of the final nanocomposites indicates that the ordered structure of the layered mineral is effectively eliminated after mixing with the polymeric mass. This means that the use of all the organo-modified clays lead to the creation of exfoliated nanocomposites where the individual clay layers loose their stacking and are uniformly dispersed in the continuous polymeric matrix. Furthermore, the broad band around 17° loose its intensity in the XRD patterns of all the nanocomposite membranes indicating changes in morphological features of the Nafion due to differences in crystallinity of the perfluorocarbon backbone. In fact, as shown in Figure S2 of the Supporting Information, this broad band can be fitted to the experimental data using two distinct diffraction peaks: a large amorphous halo centered at ca. 16°, and a superimposed Bragg peak centered at 17.5° corresponding to the crystalline fraction of the perfluorocarbon backbone.[18] The ratio between these two peaks provides a measure of the amount of crystallinity in the membrane. The crystallinity of all nanocomposite membranes is lower than that of pristine Nafion membrane indicating that the presence of modified clay nanoplatelets leads to membranes with essentially more amorphous structure.

The presence of nanofiller in the final composites was revealed also with FT-IR spectroscopy. Figure 2 shows the FT-IR spectra of Nafion−SWy/TES membrane in comparison with the filler-free Nafion, modified clay (SWy/TES), pristine clay (SWy) and TES molecule. Initially, the spectrum of the SWy/TES presents the characteristic bands of SWy and TES cations confirming the presence of organic molecules in the modified nanofiller. In addition, the pattern of Nafion−SWy/TES presents all the characteristic bands of the Nafion and the modified clay, without significant changes, confirming the presence of the organoclay (SWy/TES) in the final composite membrane. More specifically, the appearance of the peaks at 463 and 1022 cm^{-1} which correspond to Si−O and Si−O−Si vibrations of the clay lattice are indicative of the existence of the phyllomorphous mineral in the final composite. Similar spectra were observed for all nanocomposites membranes prepared using the other organo-modified clays.

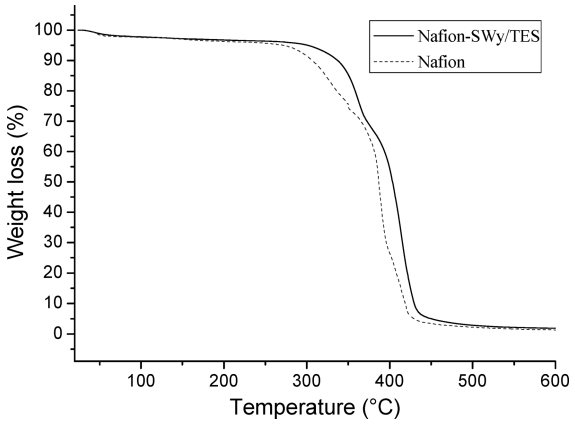

Figure 3. TGA curves of filler-free Nafion and nanocomposite membrane with 3 wt % SWy/TES.

The thermo-gravimetric curves, derived from TGA measurements, were used to determine the amount of adsorbed water in the organoclays. From the weight loss up to 120 °C, the percentage of adsorbed water was calculated for all organo-modified clays. The adsorbed water was found 7.7, 8.9, and 9.2 wt % for Lap/TES, Lap/SER, and Lap/SULF, respectively, while lower values were estimated for organo-montmorillonites, 2.5, 3.0, and 5.9 wt % for SWy/TES, SWy/SER, and SWy/SULF, respectively. The higher water content of organo-Laponite samples originates from the different structural and the physico-chemical properties of the two parent clays. In general, it is well-known[43] that Laponite clay adsorbs more water than montmorillonite (or other smectite clays) due to multilayer water adsorption on the external surface of this high surface area material. Furthermore, TGA was used also to reveal the homogeneous distribution of the organoclay platelets in the Nafion matrix. TGA results (Figure 3) show that in the case of Nafion−SWy/TES loaded with 3 wt % nanofiller, the decomposition of Nafion was shifted to higher temperatures. The higher thermal resistance of the nanocomposite than that of pure Nafion membrane is due to the strong interaction of polymer main chains with modified nanofiller which in fact provides evidence for the homogeneous dispersion of the organo-modified silicate platelets in the polymeric matrix.[42,44] Similar results were observed for all the series of nanocomposites (not shown here) indicating that all organoclay nanofillers are distributed homogenously in the polymer matrix.

3.2. Morphological Analysis. In this study, SEM was used to observe the surface morphology of the nanocomposite membranes (Figure 4) based on both SWy and Lap organoclays. Starting from Nafion−SWy (Figure 4a), the first observation concerns the difference between the superior and inferior edges (first image) as well as the two surfaces of the membrane (second image shows the superior surface): one side is smooth, compact and uniform while the other side is particularly wrinkled and spongy even if, no aggregates or agglomerates are visible inside the polymeric matrix but rather a porous structure typical of the clays. This result is imputable to the casting procedure used to prepare the membranes where, during the 8−10 h of the solvent evaporation process, the filler particles tend to settle on the substrate. In general, it is known that the preparation procedure of composite membranes by dispersion of preformed particles followed by film casting is a very simple method, but it is usually

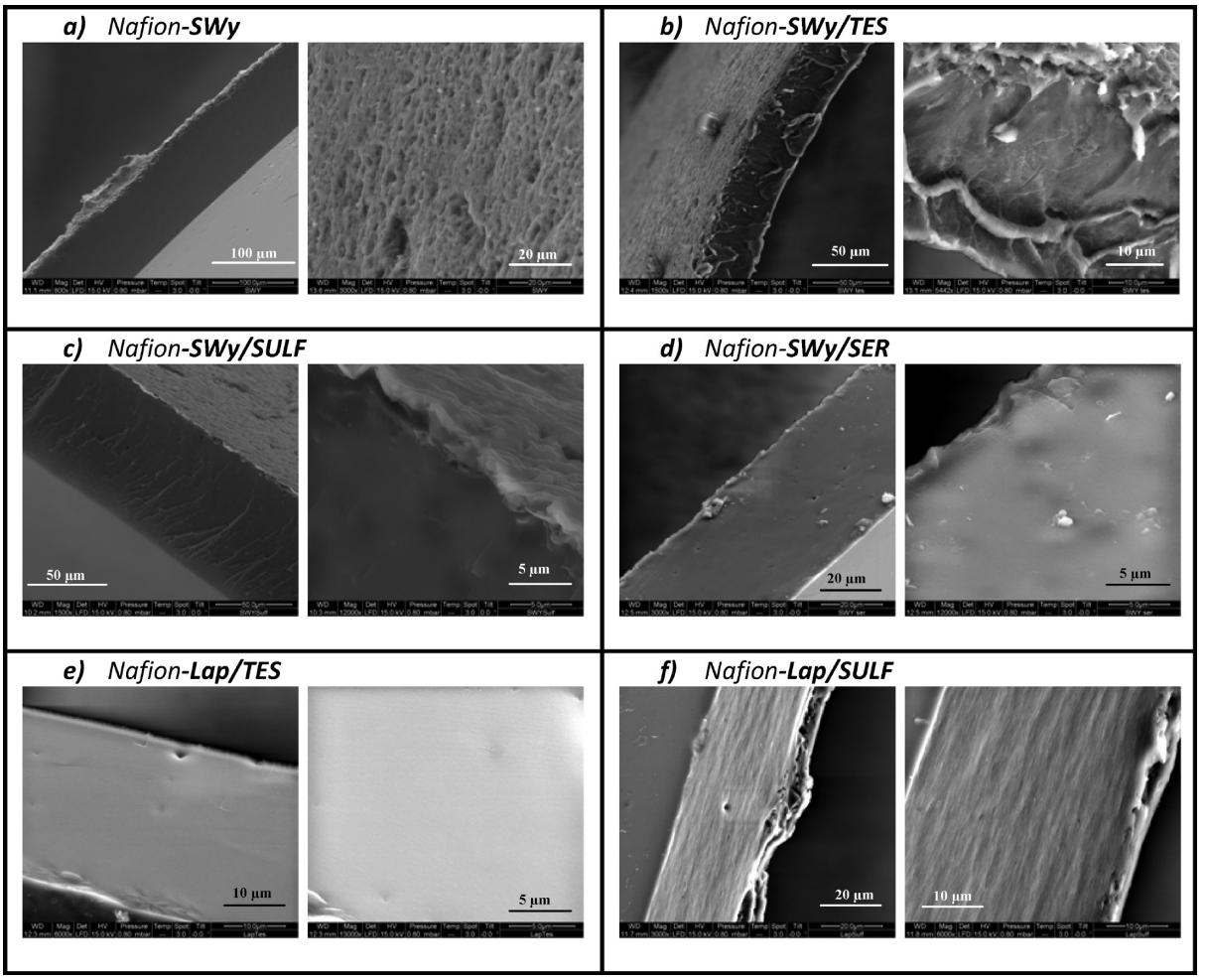

Figure 4. SEM images of the Nafion−organoclays composite membranes.

difficult to avoid the formation of particle agglomerates inside the polymeric matrix and, consequently, membranes containing nonhomogeneous dispersions of microsized particles are usually obtained.[5]

The organo-modification of the smectite clays produces some modest morphological changing in the composite membranes. In particular, SWy/TES (Figure 4b) shows a spongy structure on the entire section of the film and on both surfaces which are wrinkled even if with different intensity. Instead, SWy/SULF and SWy/SER nanocomposites show less significant changes (Figure 4, parts c and d, respectively) and have a morphology more similar to Nafion−SWy composite, with one side smooth and featureless, the other side spongy. However, going in detail, both these two nanocomposites present a structure less compact and in Nafion−SWy/SER some particles are also visible. Finally, Laponite composites show a quite different structure also by considering that the particles size is about ten times smaller than montmorillonite. Nafion−Lap/TES (Figure 4e) is uniform, smooth and homogeneous on the whole volume without pores or agglomerates, hence there is a very good dispersion of the clay platelets in the polymeric matrix. Nafion−Lap/SULF (Figure 4f), instead, shows more spongy texture with a well evident weaving and with a little deposit of clay sheets on the substrate. However,

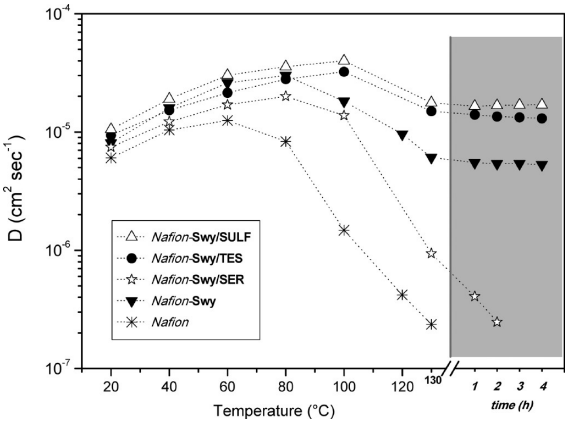

Figure 5. Self-diffusion coefficients of water confined in Nafion nanocomposite membranes based on SWy pristine clay, SWy/organo-modified clays and filler-free Nafion for comparison, from 20 °C up to 130 °C. In the graph are also plotted the data collected at 130 °C after several hours.

TGA measurements, discussed previously, have provide an evidence for the homogeneous dispersion of the organo-modified silicate platelets in the polymer, therefore, although

dx.doi.org/10.1021/jp202954g |J. Phys. Chem. B 2011, 115, 9087–9097

Table 2. Maximum Water Uptake of Filler-Free Nafion and SWy-Composites

membrane	maximum water uptake (wt %)
Nafion−SWy/SULF	50
Nafion−SWy/TES	48
Nafion−SWy/SER	35
Nafion−SWy	45
Nafion	24

a certain amount of nanofiller is deposited on the substrate (depending on the type of organoclay), the rest is evenly distributed and this will allow a vast improvement of the nanocomposite's performance compared to the filler-free Nafion.

3.3. NMR Study on SWy−Organoclays Nanocomposites. NMR self-diffusion coefficients of water confined in organo-montmorillonite composite membranes are showed in Figure 5; diffusion data of filler-free Nafion are also reported for comparison. The measurements were collected in the temperature range 20−130 °C on membranes completely swelled in pure water up to reach their maximum uptake values (these values are reported in the Table 2 for each membrane).

SWy-2 montmorillonite and its organoclays demonstrate a considerable effect on the Nafion polymer in terms both of water absorption/retention and water mobility. It is well-known, and it is corroborated also from the Figure 5, that filler-free Nafion membrane starts to lose water at about 80 °C so, at temperatures above 100 °C the conductivity go down to values no longer useful to permit the ordinary working of the cell. The presence of the clay nanofiller, both with and without surface modification, produces a noteworthy improving of the membranes performances. In fact, if we observe the water diffusion coefficients of Nafion−SWy/TES and Nafion−SWy/SULF, they increase quasi linearly up to 100 °C reaching values more than 1 order of magnitude higher than filler-free Nafion. At 130 °C is clear a slight decreasing of the diffusivity caused from the water evaporation from the membranes. However, it is extremely significant the behavior of such nanocomposites in this temperature's region since the self-diffusion coefficients remain constants for several hours at quite high values.

The reduction of the diffusivity after 100 °C, despite the increase of the temperature, can be explained by considering that the hydrophilic pores of Nafion polymer and the acid nature of the organoclay particles provide numerous proton exchange sites in the polymeric system. Therefore, the water self-diffusion coefficient measured is a weighted average from the different water species coexisting (bounded or hydrated water and bulk water[45,46]) in fast exchange rate with respect to the NMR times (see Figure S1 in the Supporting Information regarding the diffusion decay lines). In heating, it is reasonable to expect that the evaporation essentially affects the bulk/"free" water, i.e., the most mobile water so, after 100 °C, the biggest contribution to the diffusion comes from the hydrated water resulting in a lower *D*.

In any case, stating that in these measurements there is no additional humidification of the membranes, it denotes that this clay material can retain water and thus can maintain a certain level of humidity in the membrane and surface modifications with acid organic molecules significantly improve the performance of the final composite system.

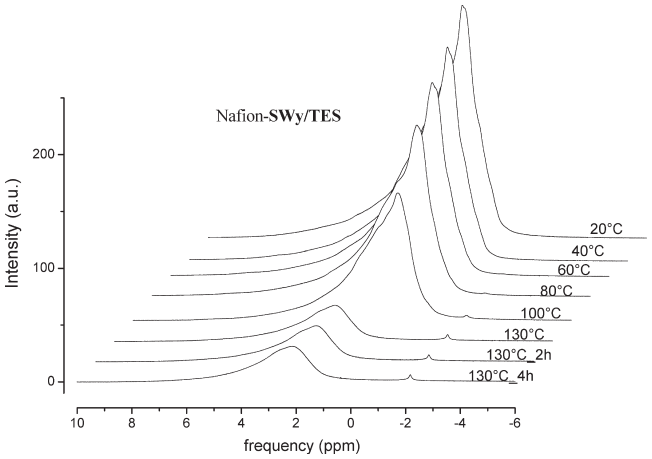

Figure 6. Temperature evolution of high-resolution ^{1}H NMR spectra of the water confined in Nafion−SWy/TES nanocomposite acquired from 20 °C up to 130 °C (at this last temperature also after 2 and 4 h).

In order to investigate on the water distribution in the membranes (hydration and bulk waters) as well as on the evaporation dynamics, we show the ^{1}H NMR spectra acquired on Nafion−SWy/TES from 20 °C up to 130 °C (Figure 6). In the graph are also reported the spectra acquired at 130 °C after 2 and 4 h, respectively. Spectra were referenced against pure water set at 0 ppm and were acquired with the same number of scans to compare their intensities. As can be seen, the proton's signal is quite large (fwhm is about 1 kHz) and asymmetric, typical of a multiple components configuration, i.e., different "types" of water coexist in the system. Actually, a certain amount of water is involved in the primary hydration "shells" of the SO_3^- groups of Nafion[47,48] as well as of the organo-modified filler's hydrophilic groups (oxygen and hydroxyl surface groups of clay and hydroxyl, amino and sulfonic groups of TES). The uptake of additional water fills the volumes of membrane's pores forming higher order hydration layers and, experiencing negligible electrostatic interactions, behaves more bulk-like. The different states of water within the hydrophilic pores can be difficult to discern because of the fast rate of proton exchange in acidic water and for this reason we "see" only one peak. The intensity of this peak decreases with increasing temperature because of the water evaporation from the membrane, with a pronounced drop above 100 °C; when it reaches 130 °C, the intensity of the residual signal remains constant for several hours (obviously without any supplying humidity), and this is responsible for the proton diffusion that we are able to detect at these high temperatures.

In all the spectra, until 100 °C, this asymmetrical signal (Figure 7A) can be fitted well to the experimental data with three Lorenzian peaks, one narrower (*peak-1*), attributed to the bulk-like water, and two broader (*peak-2* and *peak-3*), assigned to the bound water, i.e. the hydration water to the sulfonic acid groups of both the Nafion and TES molecules, and to the clay's hydrophilic groups, respectively. This peak-picking is argued from the broadness and area of the peaks: at room temperature, the amount of bulk water in completely swelled membranes is surely predominant and having less restricted molecular motions, results in a line width reduction. Furthermore, it is obvious that the water evaporation involves mainly the bulk water, in fact, at 130 °C, its contribution to the NMR signal (*peak-1*) disappear while the two broader components are still observed by peak-fitting.

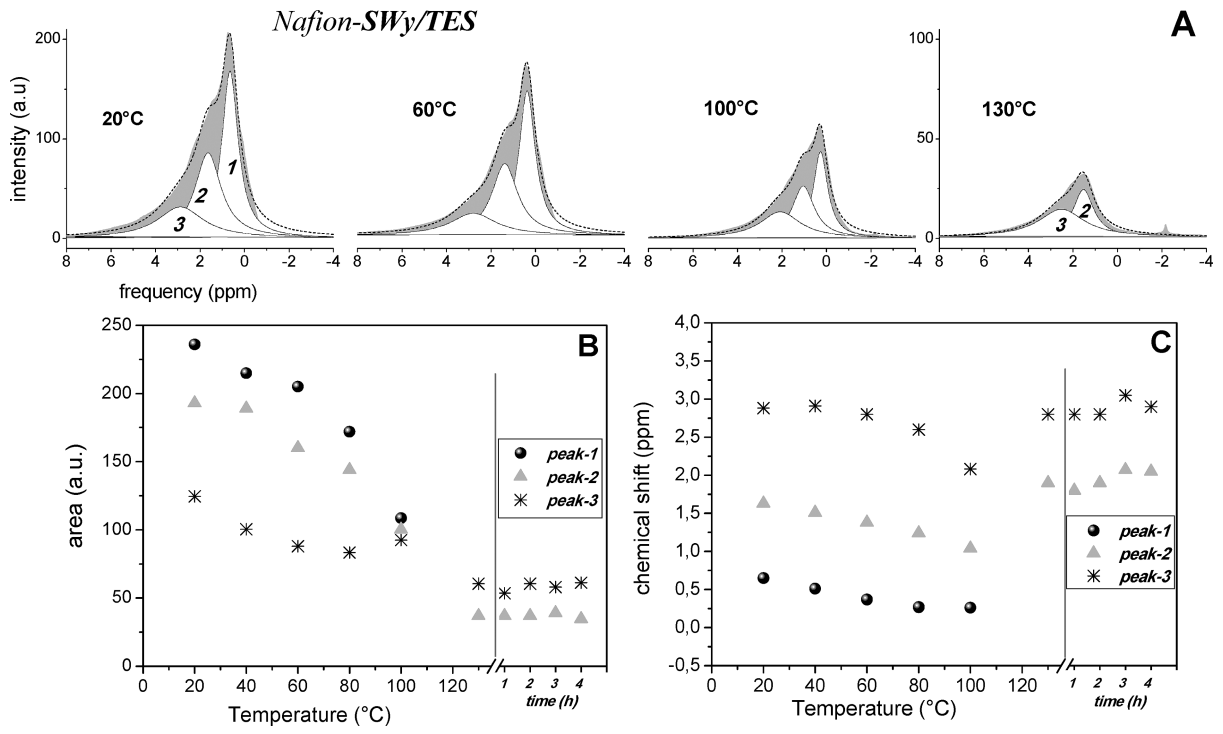

Figure 7. (A) Peak-fitting of the ^{1}H NMR spectra of the water confined in Nafion−SWy/TES nanocomposite; (B) plot of the areas of three peaks (resultants from the peak-fitting) vs temperature; (C) chemical shift of the three peaks (resultants from the peak-fitting) vs temperature.

By considering the area of these three peaks we estimate that the amount of water lost from the membrane at 100 °C is about 46 wt % of the total water initially absorbed. From this amount, 23 wt % arises from *peak-1*, 17 wt % from the *peak-2* and about 6 wt % from the *peak-3*. At 130 °C only about 18 wt % of water remains in the membrane, shared between the hydration to the SO_3^- groups of the polymer and the hydrophilic clay surfaces (*peak-2* and *peak-3*), while the bulk water is completely evaporated. The variation of the areas of these three peaks as a function of temperature is showed in Figure 7B. Up to 100 °C, the area of all signals decreases even if the *peaks 1* and 2 show a greater reduction than *peak-3* (which remains almost unchanged), while at 130 °C the proton spectrum is fitted by only two peaks (2 and 3) and their area remains constant for several hours. It is also interesting to show the trend of the chemical shift of the spectral signal, and hence of the three peaks fitting, with the temperature (Figure 7C). The reported chemical shift values were referenced to the distilled water shifts at the same temperature as the membrane. By comparing with the area's plot, a certain correspondence is noticeable: there is a downfield shift of the resonance during the heating and an abrupt change after 100 °C. This is obviously caused by the strong evaporation of water from the membrane, which in turn causes a structural change of the system (hydrophilic pores size and redistribution of water), but most likely there is also an effect due to the glass transition of the polymer (the T_g of Nafion-112 membrane is around 110 °C). However, at 130 °C the chemical shift of the signal remains invariable for several hours, indicative of the fact that no important altering, e.g., ulterior water leaking, is happening in the system.

At this point, we groped to make a quantitative analysis starting from these spectral data to estimate the number of water molecules involved in the hydration shell of the sulfonic acid groups of Nafion polymer as well as that absorbed on the organoclay nanoparticles. Taking into account the complexity of the system and to the hydrogen-bonding effects which the protons are subjected, establish the exact chemical shifts is arduous, however, by considering the concepts of electronegativity (of oxygen and sulfur atoms) and proton acidity, the resonance frequency of the protons (of the water) on the clay's surface is expected downfield shift respect to protons hydrating the sulfonic groups. Therefore, we can most likely attribute *peak-2* to the water molecules hydrating the SO_3^- groups ($h_{SO_3^-}$) and the *peak-3* to the water molecules absorbed on the organo-modified clay particles (h_{clay}).The moles of SO_3^- groups present in the Nafion/Swy-TES system originate almost entirely from Nafion and only for a negligible amount from TES molecules used to functionalize the montmorillonite clay. Even with an overestimation, i.e. by considering that the stechiometric amount of TES (which corresponds to three times the CEC of the clay) is all intercalated in the clay, and by considering the filler to polymer loading (3 wt %), this quantity is about 6% of the total moles:

$$\text{mmol of } SO_3^- = (0.2 \text{ from Nafion}) + (0.012 \text{ from TES}_{(3\text{wt\%};3\text{CEC})})$$

$$= 0.212$$

Table 3 reports a schematic description of the water distribution in the system taking into account the initial water uptake of the membrane (5.5 mmol of absorbed water) and the areas ratio of the NMR peaks at 20 °C and then at 130 °C. The hydration numbers obtained by this calculation, about 9 H_2O/SO_3^- mol/mol in the maximum hydration state and 1.8 H_2O/SO_3^- mol/mol in the very low hydration state, are in agreement with the literature;[49,50] therefore, the peak fitting and the related attributions are appropriate.

dx.doi.org/10.1021/jp202954g |*J. Phys. Chem. B* 2011, 115, 9087–9097

Table 3. Water Distribution and Hydration Numbers in the Nafion−SWy/TES Nanocomposite System

20 °C
water uptake 48 wt % → 5.5 mmol
from the areas ratio of the peaks 1, 2 and 3:
bulk 42.6 wt % → 2.34 mmol
h_{clay} 22.5 wt % → 1.2 mmol
$h_{SO_3^-}$ 34.8 wt % → 1.9 mmol ⟹ (1.9/0.212) ≅ $9H_2O/SO_3^-$ mol/mol
130 °C
∼18 wt % of the initial water uptake remain in the membrane
from the areas ratio of the peaks 2 and 3:
h_{clay} ∼ 11 wt % → 0.6 mmol
$h_{SO_3^-}$ ∼ 7 wt % → 0.38 mmol ⟹ (0.38/0.212) ≅ $1.8H_2O/SO_3^-$ mol/mol

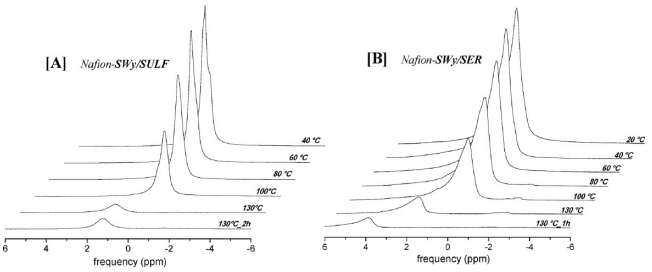

Figure 8. Temperature evolution of high-resolution ^{1}H NMR spectra of the water confined in (A) Nafion−SWy/SULF and (B) Nafion−SWy/SER nanocomposite membranes, acquired from 20 °C up to 130 °C (at this last temperature also after 2 and 4 h).

Temperature evolution of the spectra of water confined in Nafion−SWy/SER and Nafion−SWy/SULF membranes are shown in Figure 8. Once again it is visible at high temperatures, above 100 °C, the residual signal of the protons of the hydrating water the hydrophilic groups which, thanks to an appreciable mobility, can ensure the ionic transport in the membrane through, for example, the *Grotthus* mechanism, where proton mobility in water is connected to rotation of water molecules within a constantly changing network of hydrogen bonds (*structural diffusion*).[51,52]

Nafion−SWy/SULF presents the higher water uptake together with the higher self-diffusion coefficients. This excellent performance may be due, among other things, to: (i) the formation of a double-layer arrangement of the SULF molecules in the interlayer space (by XRD spectra) allowing to have a greater number of hydrophilic sites inside the polymeric system and (ii) this SWy-organofiller showed the highest capacity to absorb water (see TGA results).

The same data analysis procedure used for the spectra of Nafion−SWy/TES, gave approximately similar results in terms of hydration water to the sulfonic groups even if, in the case of SWy/SER nanocomposite we find an inferior hydration number than SWy/SULF certainly imputable to the higher water loss at 130 °C. This outcome is reflected on the diffusion and in general on the performance of the electrolyte membrane as saw in Figure 5. In fact, the rapid drop of the diffusion is hypothesized to be related to a blocking effect (the particles can obstruct the hydrophilic polymer channels) that becomes a significant factor when the water content in the membrane is very low, i.e., when the hydrophilic domains sizes are reduced.

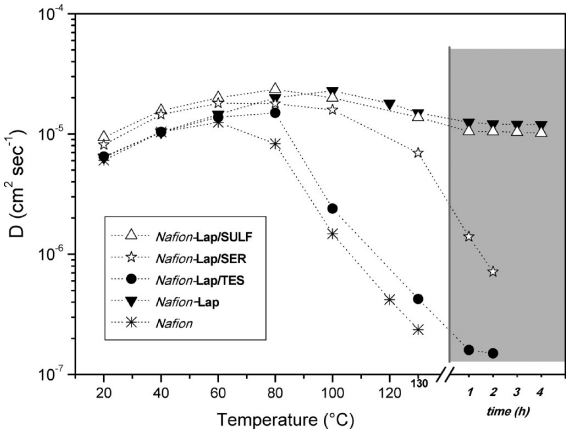

Figure 9. Self-diffusion coefficients of water confined in Nafion nanocomposite membranes based on Lap pristine clay, Lap/organo-modified clays, and filler-free Nafion for comparison, from 20 °C up to 130 °C. In the graph are also plotted the data collected at 130 °C after several hours.

3.4. NMR study on Laponite−Organoclays Nanocomposites. Concerning the organo-Laponite-based nanocomposites, the diffusion coefficients of the water confined in the various membranes are reported in Figure 9. The water uptake of all these membranes is about 30 wt % and , therefore, definitely lower than the organo-montmorillonite based membranes even if, as we reported in the TGA measurements, the water absorption of the Laponite organoclays is higher than the montmorillonites. In our view, the exfoliation that the clay platelets undergo when dispersed in the polymer matrix not only modifies their characteristic properties, but also induces an alteration on the polymeric structure. This result strengthens the idea that the structure of the composite plays a key role in the membrane performance and that the enhanced absorption is not merely a consequence of the fact that the filler's nanoparticles are more or less hygroscopic, but is also attributable to their effect on the porous structure of the polymer. However, even with a relatively low water content, the membrane prepared with pristine Laponite clay without any modification shows a good diffusion behavior in all the temperature range and it is able to preserve an excellent performance at 130 °C for several hours without any further humidification. The introduction of SULF molecules in the clay's interlayers does not improve at all the performance of the composite that, in fact, follows exactly the trend of the first one. The result is even worse when Laponite clay is organo-modified with TES and SER molecules: Nafion−Lap/SER has a collapse of the diffusion around to 130 °C, while Nafion−Lap/TES already at lower temperatures begins to show a loss of the water diffusion. Above 100 °C, practically, this reaches values comparable to those of the Nafion, although maintains a minimum water content on which we can still measure the diffusion after 2 h that it was at 130 °C. This behavior could be explained taking into account that the cationic exchange capacity (CEC) of Laponite is lower respect to SWy, therefore, the amount of organic molecules attached to the Laponite's surface is considerably lower than the correspondent organo-montmorillonites. For example the small amount of intercalated TES molecules in Laponite does not alter the hydrophilicity of the final organoclay as results from TG data: the adsorbed water which is 11 wt % in the pristine Laponite is reduced to 7.7 wt % in the case of Lap/TES. This reduction in the hydrophilicity of the nanofiller is probably

dx.doi.org/10.1021/jp202954g |*J. Phys. Chem. B* 2011, 115, 9087–9097

responsible for bad performance of the organo-Laponite Nafion membranes.

4. CONCLUSIONS

Nafion hybrid membranes based on organo-modified smectite clays were synthesized by solution intercalation and characterized by different techniques. One synthetic (Laponite) and one natural (montmorillonite) layered aluminosilicate minerals with different physical and structural properties were modified with various organic acid molecules in order to increase the concentration of hydrophilic functional groups and the compatibility with the polymeric matrix. XRD results show that fully exfoliated nanocomposites were created, where the individual organoclay layers are uniformly dispersed in the continuous polymeric matrix.

SEM analysis showed two main morphologies of the nanocomposites depending on the clay-filler used: one more smooth, compact and uniform even if there is a small deposit of filler on the substrate, the other with more wrinkled and spongy texture with a well evident weaving; however, in both case no aggregates or agglomerates are visible inside the polymeric matrix. The nanocomposite membranes with the second type of morphology showed both better diffusion performance and water retention at high temperatures.

The dynamic behavior of water confined in the nanocomposite membranes, in a wide temperature range (20−130 °C), was studied by NMR (self-diffusion and ^{1}H spectra). It was pointed out the noteworthy improving of the water retention and mobility when the organo-montmorillonites are used as fillers in the Nafion polymer. This result derives from a synergy between the hydrophilicity of the organoclays and the capacity to induce an alteration on the polymeric structure. But, the most important feature is the behavior above 100 °C: these nanocomposites can retain a small amount of " still mobile" water for several hours without any further humidification, which suggests that a significant proton conductivity can be ensured by electrolytic membranes in high temperatures condition.

Organo-Laponite fillers do not improve the electrolyte performance respect to the pristine clay without any organo-modification, this is probably due to very low amount of organic molecules able to be intercalated in this clay.

Finally, an accurate analysis of the ^{1}H NMR spectra put in evidence the different "types" of water coexisting in a composite membrane: water filling the pore volumes which behaves more bulklike, hydration water to the sulfonic acid groups of the polymer and the water absorbed on the organoclay nanoparticles.The hydration numbers obtained from these spectral data are about 9 H_2O/SO_3^- mol/mol in the maximum hydration state and 1.8 H_2O/SO_3^- mol/mol in the very low hydration state.

■ ASSOCIATED CONTENT

Supporting Information. Decay lines of $-\ln[A(g)/A(0)]$ vs g^2 which are used to calculate the self-diffusion coefficients (D), for all the temperature range explored and for the most representative membranes studied (Figure S1) and representative examples of deconvolution of the XRD diffractograms at $2\Theta = 10-24^o$ of Nafion membranes (Figure S2). This material is available free of charge via the Internet at http://pubs.acs.org.

■ AUTHOR INFORMATION

Corresponding Author

*Telephone: +39 0984 492021. Fax: +39 0984 492044. E-mail: isabella.nicotera@unical.it.

■ REFERENCES

(1) Adjemian, K. T.; Srinivasan, S.; Benziger, J.; Bocarsly, A. B. *J. Power Sources* **2002**, *109*, 356.
(2) Aricò, A. S.; Creti, P.; Antonucci, P. L.; Antonucci, V. *Electrochem. Solid-State Lett.* **1998**, *1*, 66.
(3) Adjemian, K. T.; Lee, S. J.; Srinivasan, S.; Benziger, J.; Bocarsly, A. B. *J. Electrochem. Soc.* **2002**, *149*, A256.
(4) Yang, C.; Costamagna, P.; Srinivasan, S.; Benziger, J.; Bocarsly, A. B. *Power Sources* **2001**, *103* (1), 1.
(5) Alberti, G.; Casciola, M. *Annu. Rev. Mater. Res.* **2003**, *33*, 129.
(6) Arico, A. S.; Baglio, V.; Antonucci, V.; Nicotera, I.; Oliviero, C.; Coppola, L.; Antonucci, P. L. *J. Membr. Sci.* **2006**, *270*, 221.
(7) Saccà, A.; Carbone, A.; Passalacqua, E.; D'Epifanio, A.; Licoccia, S.; Traversa, E.; Sala, E.; Traini, F.; Ornelas, R. *Power Sources* **2005**, *152*, 16.
(8) Baglio, V.; Aricò, A. S.; Antonucci, V.; Nicotera, I.; Oliviero, C.; Coppola, L.; Antonucci, P. L. *J. Power Sources* **2006**, *163*, 52.
(9) Navarra, M. A.; Abbati, C.; Scrosati, B. *J. Power Sources* **2008**, *183*, 109.
(10) Nicotera, I.; Zhang, T.; Bocarsly, A.; Greenbaum, S. *J. Electrochem. Soc.* **2007**, *154*, B466.
(11) Antonucci, V.; Di Blasi, A.; Baglio, V.; Ornelas, R.; Matteucci, F.; Ledesma-Garcia, J. *Electrochim. Acta* **2008**, *53* (24), 7350.
(12) Alberti, G.; Casciola, M.; Massinelli, L.; Bauer, B. *Membr. Sci.* **2001**, *185* (1), 73.
(13) Kongkachuichay, P.; Pimprom, S. *Chem. Eng. Res. Des.* **2010**, *88*, 496.
(14) Yano, K.; Usuki, A.; Okada, A.; Kurauchi, T. *J. Polym. Sci., Part A: Polym. Chem. Rev.* **1993**, *31*, 2493.
(15) Giannelis, E. P. *Adv. Mater.* **1996**, *8*, 29.
(16) Paul, D. R.; LM., R. *Polymer* **2008**, *49*, 3187.
(17) Chang, J.-H.; Park, J. H.; Park, G.-G.; Kim, C.-S.; O.-O., P. *J. Power Sources* **2003**, *124*, 18.
(18) Alonso, R. H.; Estevez, L.; Lian, H. Q.; Kelarakis, A.; Giannelis, E. P. *Polymer* **2009**, *50*, 2402.
(19) Wang, J.; Merino, J.; Aranda, P.; Galvan, J.-C.; E., H.-R. *J. Mater. Chem.* **1998**, *9*, 161.
(20) Ḃebin, P.; Caravanier, M.; H., G. *J. Membr. Sci.* **2006**, *278*, 35.
(21) Mbouguen, J. K.; Ngameni, E.; Walcarius, A. *Anal. Chim. Acta* **2006**, *578*, 145.
(22) Tzialla, A. A.; Kalogeris, E.; Enotiadis, A.; Taha, A. A.; Gournis, D.; Stamatis, H. *Mater. Sci. Eng. B-Adv. Funct. Solid-State Mater.* **2009**, *165*, 173.
(23) Tzialla, A. A.; Pavlidis, I. V.; Felicissimo, M. P.; Rudolf, P.; Gournis, D.; Stamatis, H. *Bioresour. Technol.* **2010**, *101*, 1587.
(24) Stathi, P.; Litina, K.; Gournis, D.; Giannopoulos, T. S.; Deligiannakis, Y. *J. Colloid Interface Sci.* **2007**, *316*, 298.
(25) Pinnavaia, T. J.; Beall, G. W. *Polymer-clay nanocomposites*; J. Wiley & Sons: New York, 2001.
(26) Giannelis, E. P. *Adv. Mater.* **1996**, *8*, 29.
(27) LeBaron, P. C.; Wang, Z.; Pinnavaia, T. J. *Appl. Clay Sci.* **1999**, *15*, 11.
(28) Zawodzinski, T. A. J.; Neeman, M.; Sillerud, L. O.; Gottesfeld, S. *J. Phys. Chem. A* **1991**, *95*, 6040.
(29) Fontanella, J. J.; McLin, M. G.; Wintersgill, M. C.; Greenbaum, S. G. *Solid State Ionics* **1993**, *66*, 1.
(30) Nicotera, I.; Coppola, L.; Rossi, C. O.; Youssry, M.; Ranieri, G. A. *J. Phys. Chem. B* **2009**, *113*, 13935.
(31) Jayakody, J. R. P.; Stallworth, P. E.; Mananga, E. S.; Zapata, J. F.; Greenbaum, S. G. *J. Phys. Chem. B* **2004**, *108*, 4260.
(32) Stejskal, E. O.; Tanner, J. E. *J. Chem. Phys.* **1965**, *42*, 288.

(33) Gournis, D.; Mantaka, A. M.; Karakassides, M. A.; Petridis, D. *Phys. Chem. of Miner.* **2001**, *28*, 285.
(34) Gournis, D.; Jankovič, L.; Maccallini, E.; Benne, D.; Rudolf, P.; Colomer, J.-F.; Sooambar, C.; Georgakilas, V.; Prato, M.; Fanti, M.; Zerbetto, F.; Sarova, G. H.; Guldi, D. M. *J. Am. Chem. Soc.* **2006**, *128*, 6154.
(35) Gournis, D.; Lappas, A.; Karakassides, M. A.; Tobbens, D.; Moukarika, A. *Phys. Chem. Miner.* **2008**, *35*, 49.
(36) MacMillan, B.; Sharp, A. R.; Armstrong, R. L. *Polymer* **1999**, *40*, 2471.
(37) Theng, B. K. G. *The Chemistry of Clay Organic Reactions*; Adam Hilger: London, 1974.
(38) de Paiva, L. B.; Morales, A. R.; Diaz, F. R. V. *Appl. Clay Sci.* **2008**, *42*, 8.
(39) Vaia, R. A.; Teukolsky, R. K.; Giannelis, E. P. *Chem. Mater.* **1994**, *6*, 1017.
(40) Gournis, D.; Mantaka-Marketou, A. E.; Karakassides, M. A.; Petridis, D. *Phys. Chem. Miner.* **2000**, *27*, 514.
(41) Mauritz, K. A.; Moore, R. B. *Chem. Rev.* **2004**, *104*, 4535–4585.
(42) Jung, D. H.; Cho, S. Y.; Peck, D. H.; Shin, D. R.; Kim, J. S. *J. Power Sources* **2003**, *118*, 205.
(43) Kaviratna, P. D.; Pinnavaia, T. J.; Schroeder, P. A. *J. Phys. Chem. Solids* **1996**, *57*, 1897.
(44) Gosalawit, R.; Chirachanchai, S.; Shishatskiy, S.; Nunes, S. P. *Solid State Ionics* **2007**, *178*, 1627.
(45) Gebel, G.; Atkins, P. *Polymer* **2000**, *41*, 5829.
(46) Paddison, S. J.; Paul, R. *Phys. Chem. Chem. Phys.* **2002**, *4*, 1158.
(47) Salles, F.; Douillard, J. M.; Denoyel, R.; Bildstein, O.; Jullien, M.; Beurroies, I.; Van Damme, H. *J. Colloid Interface Sci.* **2009**, *333*, 510.
(48) Gompper, G.; Hauser, M.; Kornyshev, A. A. *J. Chem. Phys.* **1994**, *101*, 3378.
(49) Mauritz, K. A.; Moore, R. B. *Chem. Rev.* **2004**, *104*, 4535.
(50) Falk, M. *Can. J. Chem.* **1980**, *58*, 1495.
(51) Cohen, B.; Huppert, D. *J. Phys. Chem. A* **2003**, *107*, 3598.
(52) Saito, M.; Hayamizu, K.; Okada, T. *J. Phys. Chem. B* **2005**, *109*, 3112.